Nuclear Inst. and Methods in Physics Research, A 908 (2018) 383–387

Contents lists available at ScienceDirect

Nuclear Inst. and Methods in Physics Research, A

journal homepage: www.elsevier.com/locate/nima

20 gas gaps Multigap Resistive Plate Chamber: Improved rate capability with excellent time resolution

Z. Liu [a,b,*], F. Carnesecchi [c,d], O.M. Rodriguez [a], M.C.S. Williams [b,c,e], A. Zichichi [b,c,d], R. Zuyeuski [a,d]

[a] ICSC World Laboratory, Geneva, Switzerland
[b] European Centre for Nuclear Research (CERN), Geneva, Switzerland
[c] INFN and Dipartimento di Fisica e Astronomia, Universit di Bologna, Italy
[d] Museo Storico della Fisica e Centro Studi e Ricerche E.Fermi, Roma, Italy
[e] Gangneung-Wonju National University, Gangneung, South Korea

ARTICLE INFO

Keywords:
Multigap resistive plate chamber
Rate capability
Efficiency
Time resolution

ABSTRACT

A 20 gas gaps multigap resistive plate chamber (MRPC) was built with thin (0.28 mm) glass sheets and 0.16 mm gas gap size. This chamber reaches 97% efficiency at 18.4 kV and a time resolution of 32 ps (sigma) at an instantaneous particle flux around 2.5 kHz/cm^2. Compared to a 6 gaps MRPC with 0.22 mm gas gap, this 20-gap MRPC shows a higher rate capability and much better time resolution. The efficiencies of the 20-gap MRPC reach 95%, 93% and 88% at instantaneous fluxes of 10 kHz/cm^2, 14.5 kHz/cm^2 and 20 kHz/cm^2, respectively. The efficiencies of the 6-gap MRPC at the same flux are 90%, 85% and 77%. The time resolution of 20-gap MRPC degrades with the increase of particle flux. However, a time resolution of 39 ps was obtained at an instantaneous flux of 10 kHz/cm^2.

1. Introduction

The multigap resistive plate chamber (MRPC) is often used as a time of flight (TOF) detector in nuclear and high energy experiments thanks to its very good timing characteristics [1]. Typically it has a time resolution between 50 and 100 ps [2]. At the future Compressed Baryonic Matter (CBM) experiment at Facility for Antiproton and Ion Research (FAIR) [3], the TOF detectors are required to work with a continuous flux on the order of 1–10 kHz/cm^2 for the outer region and 10–25 kHz/cm^2 for the central region [4]. Thus the rate capability is a key characteristic for the MRPCs used at the CBM experiment. The rate capability of the MRPC can be improved by using materials with lower bulk resistivity or electrodes with thinner thickness. For example, using low resistivity glass plates with bulk resistivity of 10^{10} Ωcm, a ten gap MRPC has an efficiency above 90% and a good time resolution (below 90 ps) at a flux of 25 kHz/cm^2 [5]. It is also shown that the reducing of gap size can enhance the rate capability of MRPC due to the reduction of avalanche charge [6]. In our previous studies, using a very small gas gap size of 0.16 mm, a time resolution of 20 ps was obtained [7]. Here we show the results of a 20 gas gaps MRPC with a gap size of 0.16 mm at different particle fluxes. This 20-gap MRPC is a very promising TOF detector that gives excellent time resolution and a high rate capability.

2. MRPC construction

Two MRPCs were constructed, 20-gap MRPC and 6-gap MRPC. For the convenience of comparison, both MRPCs have the same active area. The outer glass plates of two MRPCs have a dimension of 22×22 cm^2 with a 18×18 cm^2 voltage electrode; the inner glass plates have a dimension of 18×18 cm^2. All glass plates used to build both MRPCs are 0.28 mm thick and have a bulk resistivity of 1.3×10^{12} Ωcm at 24° C. The outer glass sheets were painted with resistive material to form a resistive electrode with a surface resistivity of 5 MΩ/□.

2.1. 20-gap MRPC

Fig. 1 shows the schematic of cross section of 20-gap MRPC. To simplify the construction of MRPC and reduce the number of total glass plates, the 20-gap MRPC has two stacks configuration instead of four stacks configuration as we used in [7]. Each stack is made with 2 outer glass plates and 9 inner glass plates. Fishing line, with diameter of 0.16 mm, is used to form a 0.16 mm gap size between the glass plates. A mylar sheet was placed between the voltage electrode and the printed circuit board (PCB) to isolate the high voltage. Three PCBs with pick up strips are used to readout the signals from 20-gap MRPC. The two resistive electrodes next to the middle PCB were connected with negative high voltage and the other two electrodes on the top and bottom layer connected to positive high voltage. Thus the 20-gap MRPC has two anode readout strip planes (top and bottom) and one cathode readout strip plane (middle). The width of the readout strip is 1 cm and the pitch is 1.2 cm. The length of the strip is 21 cm.

* Corresponding author at: European Centre for Nuclear Research (CERN), Geneva, Switzerland.
E-mail address: zheng.liu@cern.ch (Z. Liu).

https://doi.org/10.1016/j.nima.2018.08.096
Received 15 June 2018; Received in revised form 5 August 2018; Accepted 27 August 2018
Available online xxxx

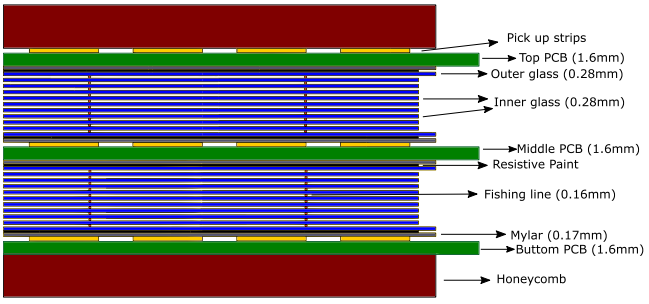

Fig. 1. Cross section of the 20-gap MRPC.

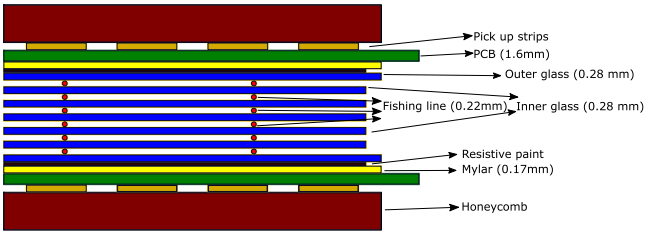

Fig. 2. Cross section of the 6-gap MRPC.

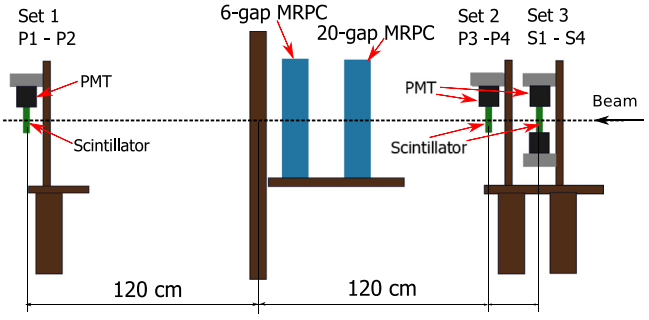

Fig. 3. The experiment setup for the MRPC test at the T10 test beam facility.

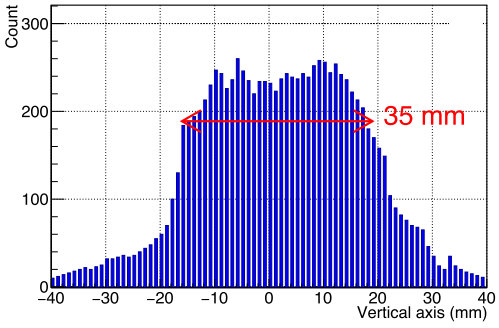

Fig. 4. The delayed wire chamber profile in vertical axis at the flux of 25 kHz/cm^2.

2.2. 6-gap MRPC

6-gap MRPC has only a single stack. Two outer glass plates and 5 inner glass plates form 6 gas gaps. The gap size of 6-gap MRPC is 0.22 mm, which is 60 μm larger than that of 20-gap MRPC. As shown in Fig. 2, the 6-gap MRPC is readout by strips located on the top and bottom PCBs. The width of the readout strip is 0.7 cm and the pitch is 0.9 cm. The length of the strip is the same as the 20-gap MRPC. Both MRPCs are supported by honeycomb and enclosed in a gas tight aluminium box.

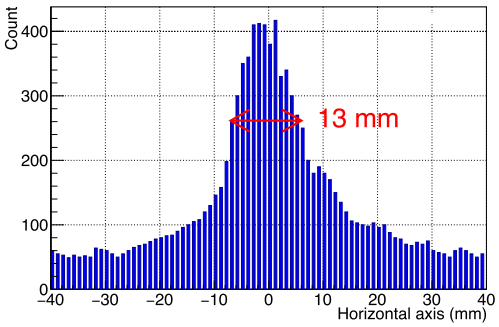

Fig. 5. The delayed wire chamber profile in horizontal axis at the flux of 25 kHz/cm^2.

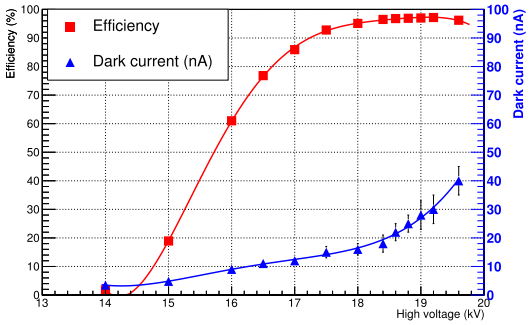

Fig. 6. The efficiency and dark current of 20-gap MRPC as a function of applied voltage with an instantaneous flux of 2.5 kHz/cm^2.

3. Experiment setup

The MRPCs were tested in T10 test beam facility at CERN [8]. Fig. 3 shows a schematic drawing of the experimental setup. The beam (mostly negative pions of 5 GeV/c momentum) had a direction perpendicular to the chamber. A gas mixture of 95% $C_2H_2F_4$ and 5% SF_6 was flowed through the chambers at a rate of 5 l/h. The size of the two scintillators of set 1 (P1, P2) is 1.2×1.2 cm^2 and set 2 (P3, P4) is 1.9×1.9 cm^2. Each scintillator of set 1 and set 2 is coupled with one photomultiplier tube (PMT). Scintillator set 3 consists of two orthogonal scintillator bars with dimension of $2 \times 2 \times 20$ cm^3. Each end of each bar is coupled to a PMT (S1, S2 for one bar, S3, S4 for the other bar). The time difference between four PMTs $((t_{S1}+t_{S2})/2-(t_{S3}+t_{S4})/2)$ has a sigma of 70 ps. This implies that the reference time of the four PMTs $((t_{S1}+t_{S2}+t_{S3}+t_{S4})/4)$ has a jitter of 35 ps. All three sets were well aligned with respect to the beam line and defined a small (1.2×1.2 cm^2) area of the beam to provide the trigger signal. The beam spill has a duration of 360 ms. By measuring the number of coincidences of set 1 and set 2 during the spill we can monitor the instantaneous flux of particles that go through the MRPCs. The beam size is measured by a wire chamber. Figs. 4 and 5 show the wire chamber profile in both vertical axis and horizontal axis at the flux of 25 kHz/cm^2. As can be seen from the wire chamber, the beam is focused on a cross section of 13 mm × 35 mm. In this spot area, the intensity varies a little. So in the small area (1.2×1.2 cm^2) we defined, the MRPC is illuminated uniformly with particles. The MRPCs were mounted on a X-Y moving table between PMT Set 1 and Set 2. This table could be positioned with a precision of 0.5 mm. By moving the table, the beam was centred in the middle of one pick up strip of the MRPC. The signals from the MRPC are discriminated by the NINO ASIC [9] and readout by WaveCatcher [10].

4. Results

4.1. Performance of MRPCs at different voltages

All results here are from T10, which has a pulsed focused beam. The flux measurement is obtained from the count rates of the scintillator sets

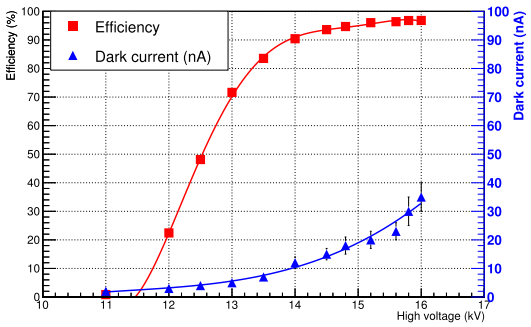

Fig. 7. The efficiency and dark current of 6-gap MRPC as a function of applied voltage with an instantaneous flux of 2.5 kHz/cm^2.

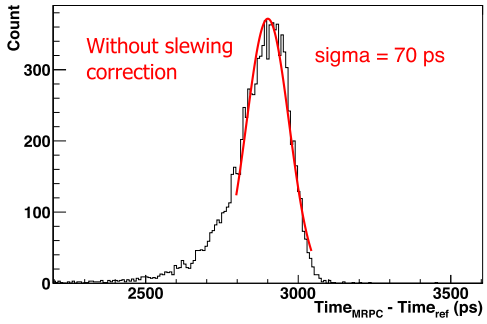

Fig. 8. Time difference between time reference PMTs (S1-S4) and 20-gap MRPC with no slewing corrections applied. The applied voltage is 18.4 kV.

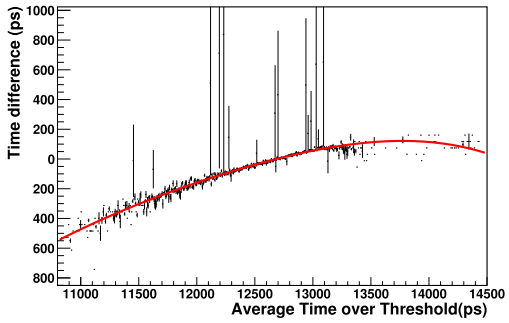

Fig. 9. Time difference between time reference PMTs (S1-S4) and 20-gap MRPC shown as a function of the pulse width. The applied voltage is 18.4 kV.

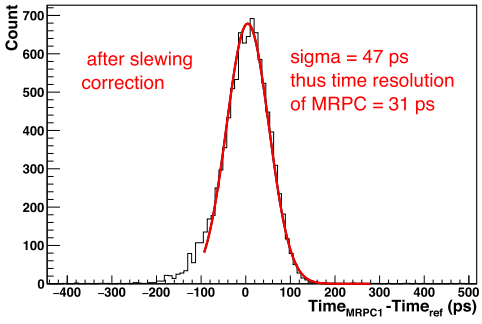

Fig. 10. Time difference between time reference PMTs (S1-S4) and 20-gap MRPC after slewing corrections. The applied voltage is 18.4 kV.

for the 360 ms spill duration. Thus the comparative performance of the two chambers at the same instantaneous flux can be examined — but

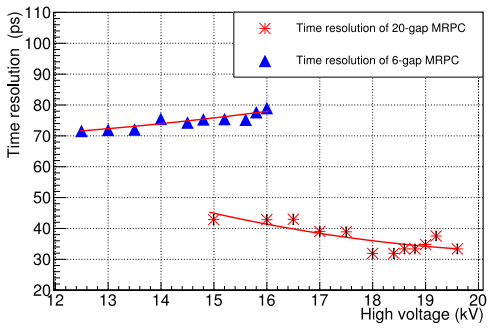

Fig. 11. The time resolution of two MRPCs as a function of voltage at 2.5 kHz/cm^2. The lines are to guide the eye.

the performance for a continuous flux of particles over the full area is difficult to evaluate.

20-gap MRPC and 6-gap MRPC have been first tested at an instantaneous flux of 2.5 kHz/cm^2 to examine their performance at different voltages. In Fig. 6, the efficiency of 20-gap MRPC for voltages between 14 kV and 19.6 kV is shown. The efficiency of 20-gap MRPC reaches a plateau at 18.4 kV. The dark current of 18 × 18 cm^2 active area of 20-gap MRPC is below 20 nA when the high voltage is below 18.4 kV and increases to 40 nA when the voltage is 19.6 kV. The efficiency and dark current as function of voltage of 6-gap MRPC is shown in Fig. 7. The efficiency of 6-gap MRPC reaches a plateau at 15.6 kV. At this voltage the dark current of 6-gap MRPC is around 20 nA.

The time of the MRPC was determined from the average time measured at each end of the strip, thus the measured MRPC time is independent of the position of the hit. Fig. 8 shows a typical histogram of the time difference for the 20-gap MRPC with respect to the time reference PMTs (S1-S4). A time resolution of 70 ps (sigma) is obtained without slewing correction. There will be time slewing dependant on the input signal amplitude since NINO chip is set at a fixed threshold for MRPC signal discrimination. The output pulse width of NINO depends on the input charge, thus we can use the pulse width information to correct the time. Fig. 9 shows a plot of the time difference as a function of pulse width; this profile is fitted by a fourth order polynomial function. The parameters of the fit are used for the slewing correction. As can be seen in Fig. 10, after correction, the time difference between the 20-gap MRPC and the time reference PMTs (S1-S4) has a sigma of 47 ps at 18.4 kV. A time resolution of 31 ps is obtained by subtracting the jitter of PMTs in quadrature. Following this time-slewing correction technique, we obtained the time resolution of 20-gap MRPC and 6-gap MRPC at different voltages, which is shown in Fig. 11. The time resolution of both MRPCs vary with different applied voltage. As the voltage increased from 12.5 kV to 15.6 kV, the time resolution of 6-gap MRPC deteriorates from 70 ps to 75 ps. The time resolution of 20-gap MRPC is much better than that of 6-gap MRPC. As can be seen in the figure, The time resolution of 20-gap MRPC is below 35 ps from 18 kV to 18.8 kV. We can conclude the 10 × 2 configuration MRPC with 0.16 mm gap size achieves better time resolution than 6 gaps MRPC with 0.22 mm gap size.

The efficiency of 6-gap MRPC reaches 96% at 15.6 kV, while the 20-gap MRPC reaches 97% at 18.4 kV. The two MRPCs are fixed at these voltages for the performance studies at different fluxes.

4.2. *The performance of MRPCs at different flux*

To test the rate capability of the MRPCs at high particle flux, we increase the instantaneous flux of particles up to 30.0 kHz/cm^2 during the beam spill. The beam spill is 360 ms long and the time between each spill is 10-20 seconds depending on the PS operation. Thus the MRPC has a long time to recover between the spills. To find out the behaviour of the 20-gap MRPC during the spills, the efficiency of the 20-gap MRPC

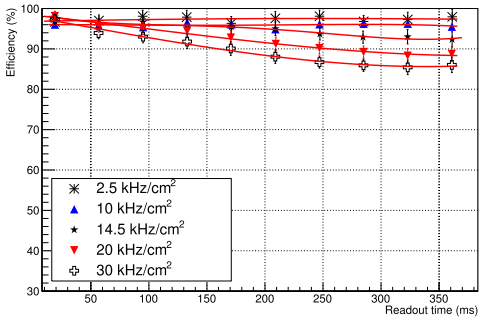

Fig. 12. The efficiency of 20-gap MRPC during 360 ms spill time. The high voltage of 20-gap MRPC is fixed at 18.4 kV.

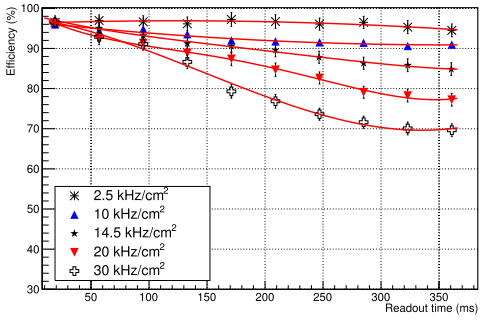

Fig. 13. The efficiency of 6-gap MRPC during 360 ms spill time. The high voltage of 6-gap MRPC is fixed at 15.6 kV.

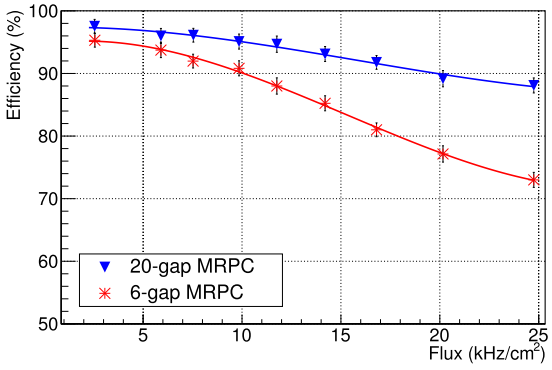

Fig. 14. The efficiency of MRPCs as a function at different flux by using only the data at the last 100 ms of the spill. The high voltage of 20-gap MRPC is fixed at 18.4 kV. The high voltage of high rate 6-gap MRPC is fixed at 15.6 kV.

for a given slice of the beam spill is plotted. The efficiency as a function of the time slice is shown in Fig. 12. As we can see, the efficiency of 20-gap MRPC is stable for the full beam spill for a flux of 2.5 kHz/cm^2 and 10.0 kHz/cm^2. However, the efficiency drops during the first half of the spill period for the flux of 14.5 kHz/cm^2 and 20.0 kHz/cm^2. When the flux reaches 30 kHz/cm^2, the efficiency looks like to be stable at 84% for the last 60 ms.

The performance of 6-gap MRPC for different particle flux is also studied. As seen in Fig. 13, the 6-gap MRPC behaves quite similar to the 20-gap MRPC for a flux of 2.5 kHz/cm^2. However, the efficiency of 6-gap MRPC sharply drops for a flux above 10.0 kHz/cm^2. The efficiency of 6-gap MRPC drops faster at higher flux than that of 20-gap MRPC. Compared to 20-gap MRPC, the efficiency of 6-gap MRPC is 15% lower at the highest flux.

As mentioned previously the flux is an instantaneous rate for a small area of the MRPC. In our analysis, to make our result closer to the continuous flux condition, we have just used the data at the last 100 ms

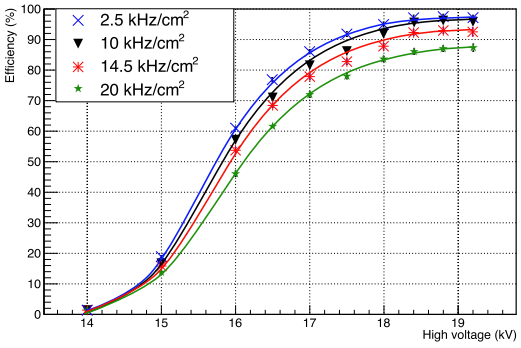

Fig. 15. The efficiency of 20-gap MRPC as a function of the voltage, at different fluxes. Only the data at the last 100 ms of the spill are used.

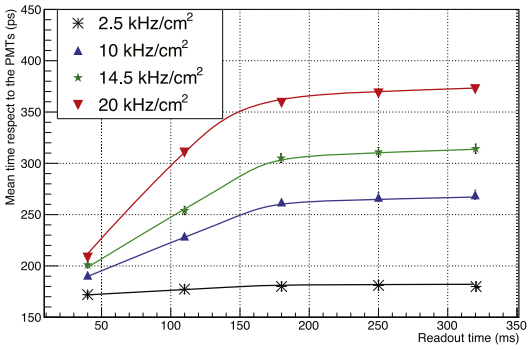

Fig. 16. The mean time of 20-gap MRPC respected to the PMTs(S1-S4) during 360 ms spill time. The high voltage of 20-gap MRPC is fixed at 18.4 kV.

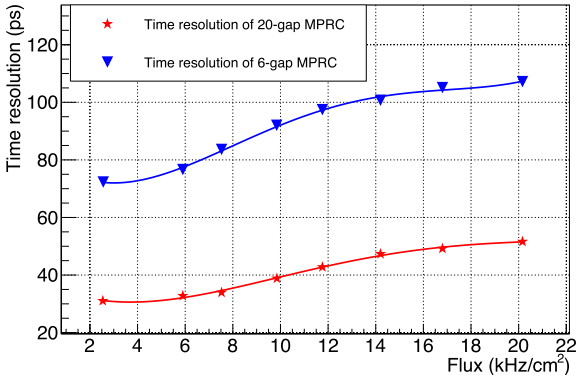

Fig. 17. The time resolution of MRPCs as a function of different fluxes. The high voltage of 20-gap MRPC is fixed at 18.4 kV. The high voltage of 6-gap MRPC is fixed at 15.6 kV. Only the data at the last 100 ms of the spill are used.

of the spill. To compare the performance of 20-gap MRPC and 6-gap MRPC, the high voltage is fixed at 18.4 kV and 15.6 kV, respectively. The efficiency of the two MRPCs as a function at different flux is shown in Fig. 14. The efficiency of 6-gap MRPC drops faster than that of 20-gap MRPC.

The performance of 20-gap MRPC with different high voltages for various particle flux is also studied. As seen from Fig. 15, the efficiency reaches the plateau at 18.4 kV for different fluxes. 18.4 kV is a good working voltage for 20-gap MRPC as an optimal voltage for high efficiency and low dark current.

We have shown at high particle flux there is a dependence between the efficiency and readout time within the spill due to the pulsed beam profile. This indicates that there is a voltage drop across the resistive plates that increases during the spill at high particle flux. To get the time

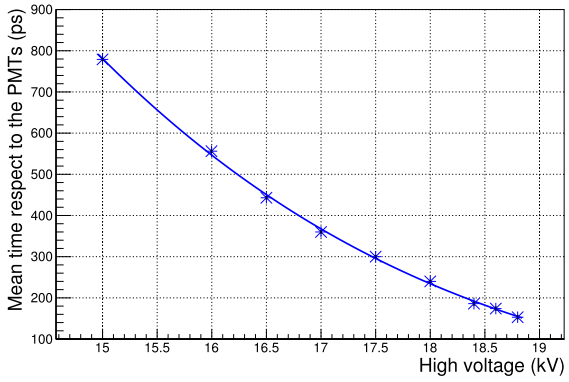

Fig. 18. The mean time of 20-gap MRPC with respect to the PMTs(S1-S4) at different voltages at 2.5 kHz/cm^2.

resolution of 20-gap MRPC in a condition equivalent to a continuous flux, the time spectra of 20-gap MRPC during the spill has been analysed and the result is shown in Fig. 16. As we can see, at instantaneous flux of 2.5 kHz/cm^2, the mean time of 20-gap MRPC is constant during the spill. However, there is a dependence when the particle flux is increased to 10 kHz/cm^2, 14.5 kHz/cm^2 and 20 kHz/cm^2. Following a similar strategy as for the efficiency, the data for only the last 100 ms of the spill are used to calculate the time resolution of 20-gap MRPC. Fig. 17 shows the time resolution of MRPCs as function of flux. As can be seen, the time resolution of both MRPCs deteriorate at higher flux. The time resolution of 20-gap MRPC is 39 ps at 10 kHz/cm^2 and 52 ps at 20.0 kHz/cm^2 and the time resolution of 6-gap MRPC is 91 ps at 10 kHz/cm^2 and 106 ps at 20.0 kHz/cm^2. The 10 × 2 gas gap configuration with small gap size of 20-gap MRPC not only gives a good time resolution in the low flux but also brings a much better time resolution at high flux than that of 6-gap MRPC.

5. Discussion

We show that the 20 gap MRPC operates well at 10 kHz/cm^2; however we should consider the case when the whole active area of the MRPC is illuminated with a constant flux of particles. Only small area of MRPC is illuminated with beam and the time of spill is short (360 ms) with a long time interval between spills of 10 to 20 seconds. For 20-gap MRPC, increasing the flux from 2.5 kHz/cm^2 to 10 kHz/cm^2 shifts the timing by 90 ps: this corresponds to a 700 V change in voltage according to Fig. 18. Using the bulk resistivity of 1.3×10^{12} Ωcm, we calculate that the total charge of each avalanche is 400 fC. This is lower (by a factor of 2 or 3) than we expected — so maybe the 10 kHz/cm^2 flux we quoted in our measurements corresponds to a continuous flux of 3 to 5 kHz/cm^2 over the full active area. However, it should be noted that the degradation of the efficiency and time resolution can be regained by increasing the applied voltage. Furthermore it should be noted that the 20 gap MRPC has a much improved behaviour at high flux than the 6 gap MRPC. To examine the actual rate capability of 20 gas gaps MRPC in a continuous flux, operating the MRPC in a long beam spill facility is planed.

Acknowledgements

The results presented here were obtained at the T10 test beam in the east hall at CERN. The authors acknowledge the support received by the operators of the PS.

References

[1] A.N. Akindinov, et al., Latest results on the performance of the multigap resistive plate chamber used for the ALICE TOF, Nucl. Instrum. Methods Phys. Res. A 533 (1) (2004) 74–78.
[2] A. Akindinov, et al., The multigap resistive plate chamber as a time-of-flight detector, Nucl. Instrum. Methods Phys. Res. A 456 (1) (2000) 16–22.
[3] Johann M. Heuser, The compressed baryonic matter experiment at FAIR, in: EPJ Web of Conferences, Vol. 13, EDP Sciences, 2011.
[4] I. Deppner, et al., The CBM Time-of-Flight wall: a conceptual design, J. Instrum. 9 (10) (2014) C10014.
[5] Jingbo Wang, et al., Development of multi-gap resistive plate chambers with low-resistive silicate glass electrodes for operation at high particle fluxes and large transported charges, Nucl. Instrum. Methods Phys. Res. A 621 (1–3) (2010) 151–156.
[6] K.S. Lee, et al., J. Instrument P10009 (2012).
[7] S. An, et al., A 20 ps timing device - A Multigap Resistive Plate Chamber with 24 gas gaps, Nucl. Instrum. Methods Phys. Res. A 594 (1) (2008) 39–43.
[8] http://sba.web.cern.ch/sba/BeamsAndAreas/East/East.htm.
[9] F. Anghinolfi, et al., NINO: an ultra-fast and low-power front-end amplifier/discriminator ASIC designed for the multigap resistive plate chamber, Nucl. Instrum. Methods Phys. Res. A 533 (1) (2004) 183–187.
[10] D. Breton, J. Maalmi, E. Delagnes, Using ultra fast analog memories for fast photodetector read out, NDIP 2011, Lyon.